Challenges in Ground-Penetrating Radar Application in Structural Elements: Determination of the Dielectric Constant of Glued Laminated Timber Case Study

Varevac, Damir; Guljaš, Ivica; Ištoka Otković, Irena; Radočaj, Dorijan

Source / Izvornik: **Electronics (Basel), 2024, 13**

Journal article, Published version
Rad u časopisu, Objavljena verzija rada (izdavačev PDF)

https://doi.org/10.3390/electronics13183718

Permanent link / Trajna poveznica: https://urn.nsk.hr/urn:nbn:hr:133:573575

electronics

MDPI

Article

Challenges in Ground-Penetrating Radar Application in Structural Elements: Determination of the Dielectric Constant of Glued Laminated Timber Case Study

Damir Varevac [1], Ivica Guljaš [1], Irena Ištoka Otković [1] and Dorijan Radočaj [2,*]

[1] Faculty of Civil Engineering and Architecture Osijek, Josip Juraj Strossmayer University of Osijek, Vladimir Prelog St. 3, 31000 Osijek, Croatia; dvarevac@gfos.hr (D.V.); iguljas@gfos.hr (I.G.); iirena@gfos.hr (I.I.O.)

[2] Faculty of Agrobiotechnical Sciences Osijek, Josip Juraj Strossmayer University of Osijek, Vladimir Prelog St. 1, 31000 Osijek, Croatia

* Correspondence: dradocaj@fazos.hr; Tel.: +385-31-554-879

Abstract: In this paper, some of the basic information on Ground-Penetrating Radar (GPR), its applications (especially in the field of civil engineering) and limitations are presented. As a non-destructive technique, GPR is a powerful tool for the investigation of structures and structural members, roads, geological layers, archaeological sites and many more. The technology is based on electromagnetic radiation in the UHF/VHF range (10 MHz to 3 GHz). The choice of the frequency depends on the intended use, depth and size of the target and medium where the target is located. Joined with other testing methods (ultrasound method, dynamic methods with forced or ambient vibrations, electrical conductivity testing, etc.), GPR can provide a deep insight into the investigated object. However, like many other non-destructive methods, the choice of input parameters may affect the results. In this regard, a case study presented in this paper demonstrates not only different applications of GPR in civil engineering but also the determination (calibration) of one of those input parameters: the dielectric constant of glued laminated timber. The challenge here was not only to investigate the influence of the direction of measurements with regards to the direction of the fibers but also to acknowledge the contribution of the test antenna used during testing and dielectric constant calibration.

Keywords: Ground Penetrating Radar; receiver and transmitter; central frequency; electromagnetic waves; propagation velocity; dielectric constant; radargram; range depth; resolution; target size

Citation: Varevac, D.; Guljaš, I.; Ištoka Otković, I.; Radočaj, D. Challenges in Ground-Penetrating Radar Application in Structural Elements: Determination of the Dielectric Constant of Glued Laminated Timber Case Study. *Electronics* **2024**, *13*, 3718. https://doi.org/10.3390/electronics13183718

Academic Editors: Toshifumi Moriyama and Fei Wang

Received: 23 July 2024
Revised: 1 September 2024
Accepted: 17 September 2024
Published: 19 September 2024

1. Introduction

Georadar (Ground-Penetrating Radar or GPR) is a method that uses radar technology to investigate hidden or inaccessible, usually buried, items, structures or layers. This method is in the group of non-destructive methods, and its applications are very wide: pavement survey, preliminary analysis of ground characteristics, detection of buried items, rebar detection in concrete structures, detection of underground cavities or road bed voids, utilities detection, critical analysis of structures, checking of structures after rehabilitation, archaeological survey, etc. [1].

The idea itself reaches back to the first half of the 20th century, and the first patent was in Germany [1]. Full application of the radar technology occurred in WW2, and since then the development in military and civil fields has been rapid. GPR can be used in a variety of media, including rock, soil, ice, fresh water, pavements and structures. It can detect objects, changes in material, voids and cracks. At the inception of GPR technology, it was primarily applied to natural grounds, though now it is a well-accepted technique to investigate any kind of material, such as wood, ice, concrete, asphalt, etc. [2–11].

The dielectric constant is critically important to obtaining accurate depth readings with GPR systems. Dielectric constants, also known as relative dielectric permittivity, are

measured on a scale of 1 to 81, where 1 is the dielectric constant for vacuum (through which radar waves travel most quickly) and 81 is the constant for water (through which radar waves travel most slowly). Of course, one can also assume the value of 1 for air and keep in mind that water temperature and its salinity can influence the actual numbers. Nevertheless, those values are more than good enough, at least in the initial phase of measurements. Metallic objects that could be considered as perfect reflectors exist outside the scale, since radar waves cannot penetrate them at all; they are described as having an infinite dielectric constant. In order to convert the variable that is produced by a radar reading—time—into the desired product of the reading—depth—GPR systems must be accurately programmed with the correct dielectric constant for the ground material in question. This enables GPR systems to produce meaningful depth readings, instead of timed reflection readings; these timed reflection readings are transformed in an equation with the proper dielectric constant. As a result, depth readings from GPR systems are only as accurate as the dielectric constant with which they are programmed for each particular ground material. Given this, it is no wonder that dielectric constant assessment is a very important part of GPR technique promotion and further applications ranging from general theoretical models and methods to a variety of experimental validations in various heterogeneous and anisotropic materials and structures ranging from concrete, wood and pavements up to biomass [12,13].

This is especially the case for glulam (Glue Laminated Timber—GLT) load-bearing elements. Glulam is a natural structural material made from laminates of timber glued together under heat and pressure. Such load-bearing elements have a high load capacity, do not have a problem with corrosion and have a high resistance to fire. The disadvantage of this material lies in its natural origin. In addition to being anisotropic, i.e., having different mechanical properties in different directions, it is subject to defects that can have a major impact on load-bearing capacity. These defects can be cracks, knots, shakes or tunnel-like holes from insects. The detection of these irregularities within the structural element is of great importance, so georadar is an excellent solution. However, due to the size of these irregularities, which ranges from approximately 0.5 cm to 5.0 cm, the selection of the antenna, i.e., its central frequency, is particularly important. High-frequency antennas (1 GHz and higher) must be used to detect such small targets.

2. Fundamentals of Georadar

This non-destructive method uses electromagnetic (EM) radiation in the microwave band (UHF/VHF frequencies) of the radio spectrum, and it detects the reflected signals from subsurface structures. Electromagnetic radiation is in the form of a series of short pulses emitted from antennas into the ground. When the wave hits a buried object or a boundary with different dielectric constants, the receiving antenna records variations in the reflected return signal. One part of the wave is refracted and continues its travel in the ground; another part is reflected and comes back to the surface. It is the reflected signal that is recorded when it gets back to the surface (Figure 1a).

Basically, the parameter that determines the amplitude and frequency of the return signal mostly depends on the already mentioned dielectric constant. Even within the same material, in the case of changed conditions, such as changes in humidity or changes in density, the dielectric constant, and thus the reflected signal, changes. The greater the difference in the value of the dielectric constant, the greater the contrast and thus the better the visibility of the target.

Figure 1b shows the radar trace for one particular position of the transmitter/receiver, and Figure 1c is the data record obtained by moving with the equipment over the surface. For each position of the system, an EM wave is emitted and reflection is recorded. The associated time between emitting and receiving the signal, along with its energy, are stored for post-processing and visual representation. In order to transform time data [ns] into depth [m], the velocity of the EM wave should be known. This propagation velocity may

be determined approximately (by neglecting the influence of the conductivity, σ) by the Equation (1):

$$v = \frac{c_0}{\sqrt{\varepsilon_r \mu_r}} \quad (1)$$

or, assuming that the relative magnetic permeability μ_r is close to unity:

$$v = \frac{c_0}{\sqrt{\varepsilon_r}} \quad (2)$$

where:

v propagation velocity of EM wave in the media
c_0 EM wave velocity in vacuum ($3 \cdot 10^8$ m/s)
ε_r relative permittivity
μ_r relative magnetic permeability.

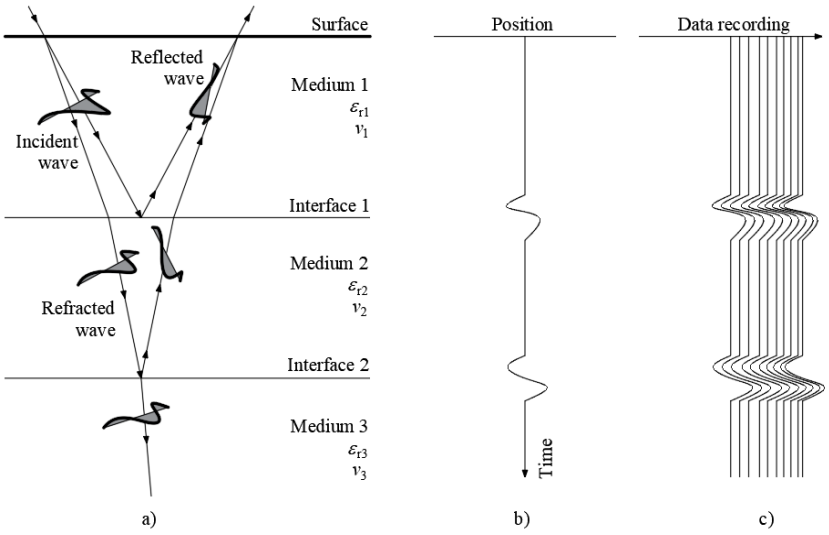

Figure 1. Basic principles of georadar: (**a**) Behavior of EM waves in layered media; (**b**) radar trace; (**c**) data recording.

Time-to-Depth conversion is crucial for locating the target under the surface, whether it is an object or layer. The estimation of the propagation velocity v in a single-layered medium is usually a relatively simple task, but for a multi-layered medium it is more complex. The detailed velocity model is the most accurate, but its drawback is invasiveness. This model assumes that core samples are taken and the propagation velocity for each layer is assigned [14,15]. Other methods, which use GPR data only, are not accurate, but in most cases the results are satisfactory.

The most frequently used ones are the Common Midpoint Method and Hyperbolic Velocity Analysis [14,15]. Hyperbolic Velocity Analysis is used for Time-to-Depth conversion (Figure 2). In the case where there is a clear hyperbolic response on the radargram, hyperbola fitting can be used to calculate the speed of the radar signal. The angle of the arms of the hyperbola is directly related to the speed: the wider the angle, the higher the velocity, and vice versa. In Figure 3, the radargram after Time-To-Depth conversion is shown.

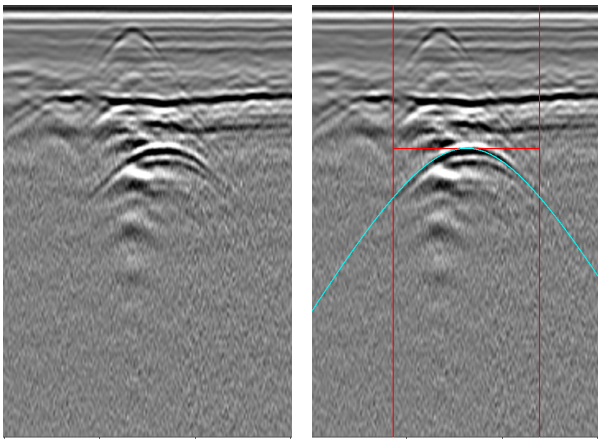

(**a**) (**b**)

Figure 2. Hyperbolic velocity analysis for Time-to-Depth conversion. (**a**) Radargram containing hyperbolic shape. (**b**) Hyperbola fitting.

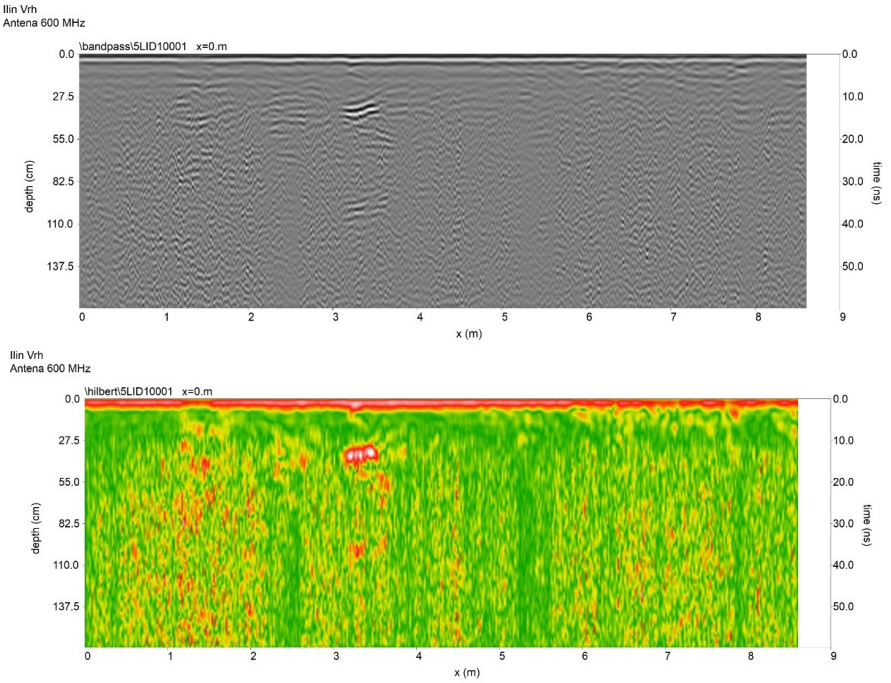

Figure 3. Radargram recorded at archaeological site "Ilin vrh" after Time-to-Depth conversion, bandpass filtering (**above**) and Hilbert transformation (**below**).

3. Some Practical Issues in Georadar Application

In the previous consideration of the basic principles of GPR technology, only the main parameters affecting the application are shown. The end user should not have elaborate physics skills to make use of the georadar, but one must be familiar with some guidelines that increase or decrease georadar performance. Some elementary questions will be explained in the following text.

3.1. How Deep Can One See?

The range of GPR (depth) depends on many parameters. Generally, the performance of GPR may be estimated from radar Equation (3):

$$Q = 10 \cdot \left(\frac{P_{min}}{P_t} \right) \, [dB] \tag{3}$$

where

P_{min} minimum detectable power of the receiver;
P_t transmitter output power.

The ratio $\frac{P_{min}}{P_t}$ can be calculated from the following expression:

$$\frac{P_{min}}{P_t} = \frac{E_t E_r G_t G_r v_m^2 g e^{-4\alpha R} \sigma}{64\pi^3 f^2 R^4} \quad (4)$$

where:

E_t and E_r antenna efficiency (transmitter and receiver, respectively)	System-dependent
G_t and G_r antenna gain	
f central frequency of antenna	
v_m propagation velocity	Media-dependant
α attenuation coefficient of medium	
g scatter gain of target	Target-dependent
σ target scattering cross-section area	
R distance to the target	Range-dependent

As can be seen from expressions (3) and (4), the GPR user has control over some parameters (system-dependent) by choosing the right configuration of the georadar—usually the central frequency of the antenna. Other parameters are out of the user's control, and they depend on site-specific conditions. Without going deeper into these equations, some general rules apply, as follows [16,17].

The range (depth) of GPR decreases proportionally to the increase of the electrical conductivity of the medium, water content, clay content, scattering, conductive contaminant, but it increases with receiver sensitivity, transmitter power and is inversely proportional to the frequency (Table 1). Figure 4 shows the difference in range depth for the 600 MHz and 200 MHz antennas. It can be seen that the 600 MHz antenna provides a more precise record, but it penetrates to approximately 150 cm in depth, while the 200 MHz antenna has a range depth of over 300 cm. The recommended frequencies of the antennas, along with the range depth and intended use, are shown in the table below.

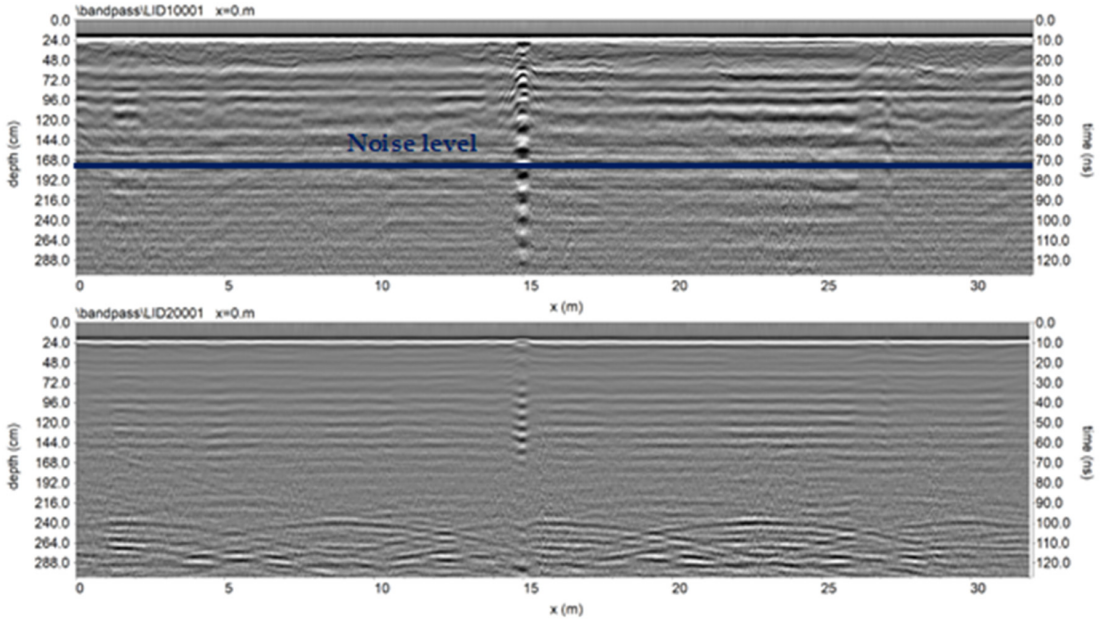

Figure 4. Radargram recorded at Đakovo cathedral with 600 MHz antenna (**above**) and 200 MHz antenna (**below**).

Table 1. Recommended central frequencies of the antenna for intended use [17].

Center Sample Frequency [MHz]	Application	Range	
		Depth [m]	Travel Time [ns]
16–80	Geologic	5–30+	400–800
80	Geologic	5–30	300–700
100	Geologic Environmental	4–25	300–500
200	Geologic Environmental	1–10	70–300
300	Shallow Geology Environmental	1–9	70–300
400	Shallow Geology Environmental	0.5–4	20–100
500	Shallow Geology Environmental Archaeology	0.5–3.5	20–80
900	Concrete, Soils Archaeology Engineering Structures	0–1	10–20
1000–3000	Concrete Pavements Bridge Decks	0–0.5	10–15

3.2. What Accuracy Can Be Expected?

Locating the target within the medium assumes positioning the point of interest in both horizontal (x) and vertical (y) directions. It is necessary to establish a coordinate system where the horizontal axis lays at the surface of the medium (for example, a bridge deck or road pavement) and the vertical axis is perpendicular to it. Usually, the horizontal location is determined by either connecting the georadar system to GPS station, which links GPR data with the geographic location, or by a metric (survey) wheel, which is mounted to the antenna. With proper planning and care during the acquisition phase, an accuracy of a few centimeters can be assured. As discussed before, determining the vertical coordinate (depth of the target) demands more effort. The depth of the target is calculated from a time of flight of the electromagnetic waves from the antenna to the target and back (so-called 2-way travel time). Inaccuracies may arise due to the time/depth conversion process, which requires an accurate evaluation of the propagation velocity in the medium. Choosing a wrong value for the propagation velocity largely affects the vertical accuracy. According to the simplified Equation (3), propagation velocity depends on the dielectric constant of the media. Additionally, since the georadar uses an encoder to measure distances, the errors could be due to the errors inherent to the encoder itself. Estimated dielectric constants for various typical media, shown in Table 2, may serve as a guidance.

If a great degree of accuracy is needed, the best way to achieve this is to calibrate the measurements against targets with a known depth. This can be achieved either by burying the target to a known depth or by control measurement.

Table 2. Estimated dielectric constants ε_r for typical media [18,19].

Medium	ε_r	Propagation Velocity v [cm/ns]
Air	1	30
Water	81	3
Sand	2.6–25	19–6
Silt	2.5–19	19–7
Clay	2.4–15	19–8
Wet basalt	8	11
Wet granite	7	11
Wet sandstone	6	12
Wet limestone	8	11
Concrete	7	13
Asphalt	3	14

3.3. What Horizontal and Vertical Resolution Can Be Achieved?

Horizontal resolution is the capability of the radar to distinguish close targets at the same depth. It could be considered as the ability of the system to detect lateral changes along the survey path. Since the radar antenna transmits a cone of energy into the subsurface, the majority of the reflected energy comes from the central area of the cone, called the first Fresnel zone. The best results are achieved if all targets fall into the first Fresnel zone, so the radius of that zone dictates plan resolution. Vertical resolution, or depth resolution, is the capability to distinguish between the various targets in the depth range. Technically, it is the ability to differentiate two adjacent targets along the time axis [20].

These properties depend on the wavelength and bandwidth of the antenna, radar acquisition parameters, medium and target properties, so no definite answer can be given, but the general rule is that a higher GPR antenna frequency results in a better resolution, both vertically and horizontally.

3.4. What Is the Minimum Target Size?

The minimum detectable target size is related to the so-called Radar Cross Section, which depends on the material of the target and medium, but there are physical limitations as well. Neglecting the site-specific conditions, the minimum size of the target is governed by the properties of the EM wave, i.e., its wavelength:

$$\lambda = \frac{v}{f}\ [m] \tag{5}$$

where

λ wavelength in [m]
v propagation velocity of EM wave in the media in [m/ns]
f central frequency of antenna in [GHz].

Most researchers agree that the theoretical lower limit for a target to be detectable is 10% of the wavelength [8]. This implies that the higher the frequency of the antenna (and the lower the propagation velocity), the smaller the target that can be detected. Using the propagation velocities from Table 2 and Equation (5), one can easily calculate the minimum target size for different media (Table 3).

The data provided in Table 3 should be taken into consideration very carefully. Considering the radar cross section, material of the target and parameters of the soil, the real minimal size of the target may be 5 to 10 times larger than the provided values. Beside this fact, Table 1 implies that the price for detecting a smaller minimum target size would be paid in range depth: the smaller the detectable target size, the smaller the range depth.

Table 3. Theoretical minimal size of the target depending on medium and central frequency of the antenna.

Medium	Propagation Velocity [m/ns]	Wavelength λ [m] for Central Frequency			Min. Target Size [cm]
	v	f = 600 MHz	f = 1.0 GHz	f = 3.0 GHz	0.1 λ
Concrete	0.13	0.216	0.130	0.043	2.1/1.3/0.4
Asphalt (dry)	0.14	0.233	0.140	0.046	2.3/1.4/0.6
Clay (dry)	0.19	0.316	0.190	0.063	3.1/1.9/0.6
Sand (wet)	0.06	0.100	0.060	0.020	1.0/0.6/0.2
Water (fresh)	0.81	1.350	0.810	0.270	13.5/8.1/2.7

4. Some of Our Own Case Studies in Georadar Application

Our intention, besides a case study on glued laminated timber structures presented in the following chapter, was to share our long-term experience in GPR methodology application in structural engineering. We have tried (and still trying) to improve what we have learned during our basic education in that field by learning from every single particular assignment, task and practical problem. We are aware that proper skills in application and in results interpretation, especially directly on field tests, rely on previous case studies and experience. That is the reason why we added this second chapter in order to emphasize our journey to the phase where we are not just the followers of the defined rules but are also able to question and eventually improve some basic input parameters needed for better and more reliable results.

Here are some of the interesting GPR surveys conducted by the Faculty of Civil Engineering and Architecture Osijek. The GPR equipment used in all surveys is manufactured by IDS GeoRadar s.l.r (Pisa, Italy), using 200 MHz, 600 MHz, 900 MHz and 2.0 GHz antennas. These surveys also demonstrate possible applications of georadar and its power in civil and structural engineering.

4.1. Jean-Michel Nicolier Bridge in City of Vukovar

The pedestrian bridge "Jean-Michel Nicolier" is located in the center of the town Vukovar over the river Vuka. Each year, Remembrance Procession is held, and, at the time, almost 100,000 people walk over in tight formation.

Although there are no records on bridge construction, it was probably built in the 1950s. The total length is 29.80 m consisting of three spans (9.00 + 11.80 + 9.00 m). Two piers support a reinforced concrete slab, originally 55 cm thick. Together, they are intended to form a monolithic frame structure simply supported at abutments. At first glance, the bridge appears to be in good shape, but on closer visual inspection critical faults were found. The concrete cover from the bridge soffit (undersurface) fell off, the reinforcement in the lower zone is completely exposed, and no bond between the rebars and concrete exists (Figure 5).

Figure 5. Damage of the superstructure soffit.

The survey of the span in the longitudinal direction was carried out in five sections. It clearly shows the layers of superstructure (stone lining, several layers of concrete). Within the concrete body of the slab, no large cracks or cavities were observed, so it can be considered to be in a relatively good condition. The transverse reinforcement is located at a depth of 25–28 cm at intervals ranging from 24 to 30 cm in the midspan and 15 to 21 cm above the piers. The main longitudinal reinforcement in the upper zone is also unevenly distributed. It is located at a depth of 21 to 27 cm and at intervals ranging from 12 to 20 cm (Figure 6).

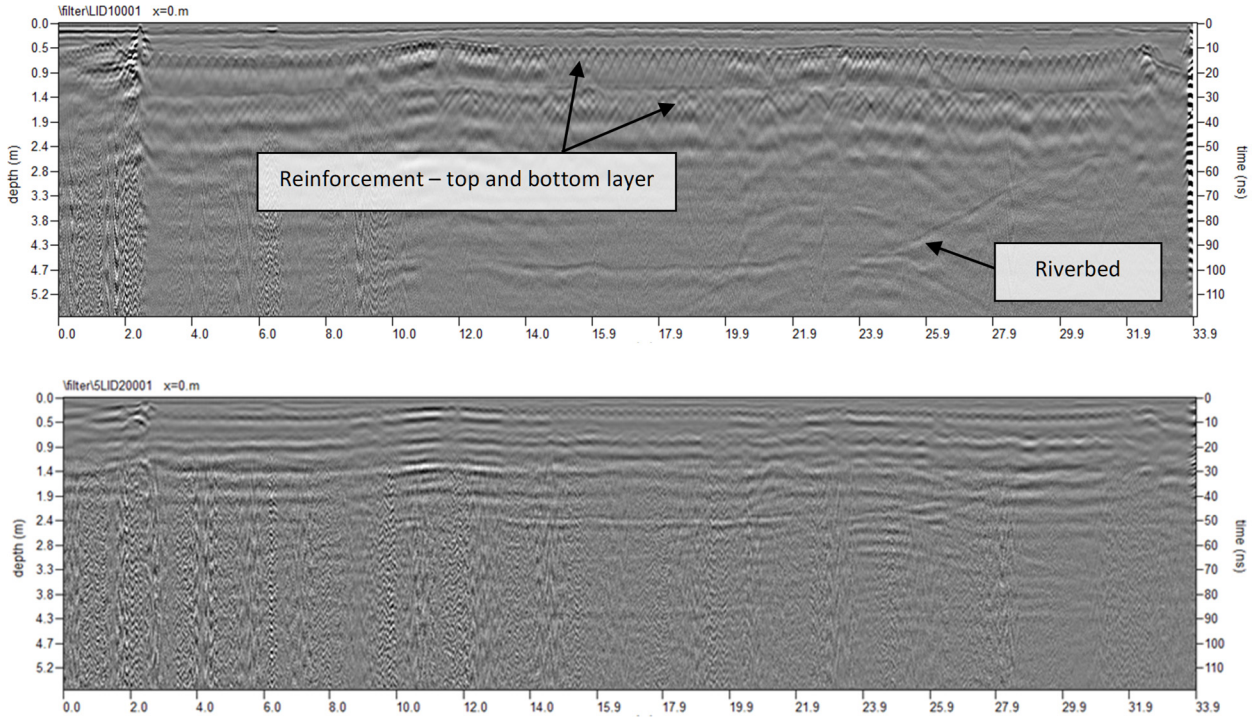

Figure 6. Radargram of the RC slab in the longitudinal direction: 600 MHz antenna (**above**) and 200 MHz antenna (**below**).

4.2. Church of St. Andrew Apostle in Viljevo

According to the schematics of Roman Catholic Bishoprics of Pécs, the church of St. Andrew Apostle in Viljevo, eastern Croatia (Figure 7) was built in 1280. Since then, it was rebuilt several times in the 18th and 19th century. Although well documented since the 13th century, historians suspect that the foundation of this church dates even back to the 11th century.

Figure 7. The Church of St. Andrew Apostle in Viljevo, Croatia.

The aim of this survey was to determine if the remains of old foundations might be found. Additionally, it was decided to verify the structural integrity of the walls using GPR technique. Figure 8 shows the layout of the church with the scan path on the floor (left) and the findings (right). For this survey, 200 MHz and 600 MHz antennas were used.

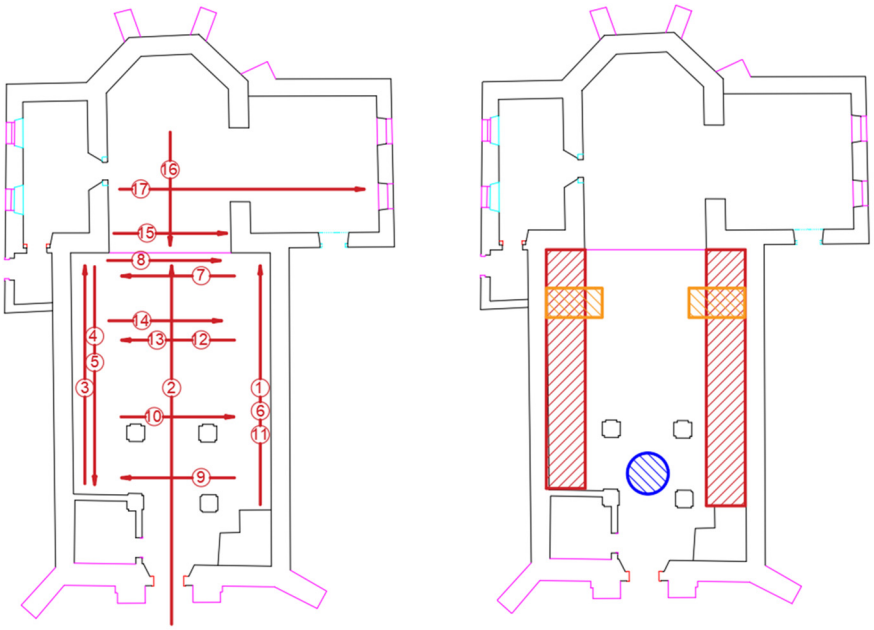

Figure 8. The layout of the church with the scan path (**left**) and recorded remains of old foundations (**right**).

The GPR survey confirmed the presence of previous foundations within the church (marked orange and red on Figure 8) at a depth of approximately 50 cm below the floor. The corresponding radargram for scan No. 1 is shown in Figure 9.

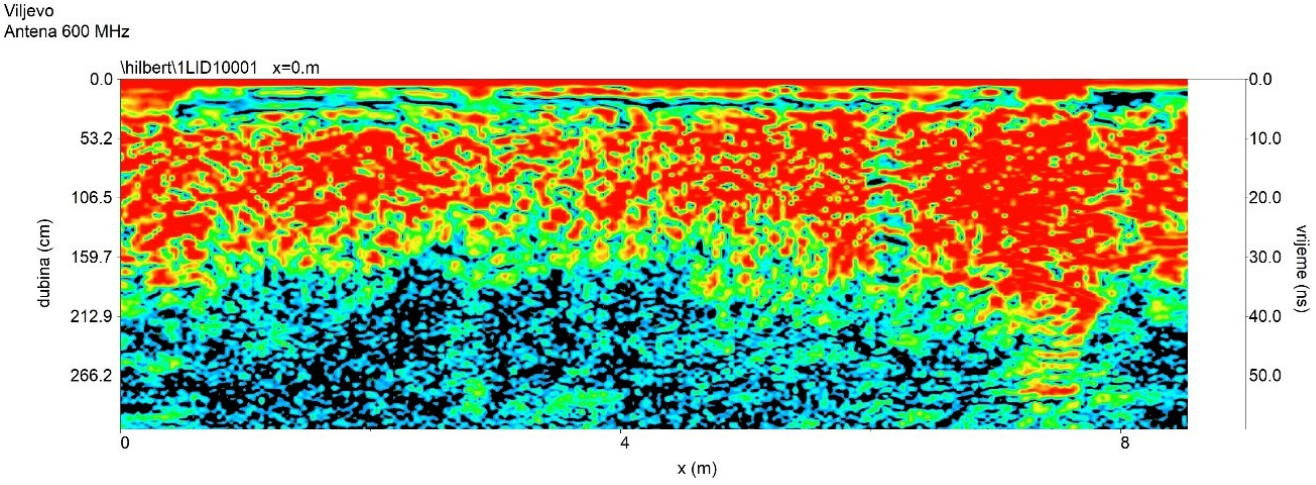

Figure 9. Radargram recorded at scan line No. 1 after Time-to-Depth conversion, bandpass filtering and Hilbert transformation—600 MHz antenna.

A very interesting response was obtained at scan line No. 2 (position marked with a blue circle on Figure 8, right). At a depth between 100 and 150 cm, the anomaly is recorded (Figure 10). Since the soil in this region is mostly homogeneous and free of rock or boulders, there is a high probability that it is a buried item.

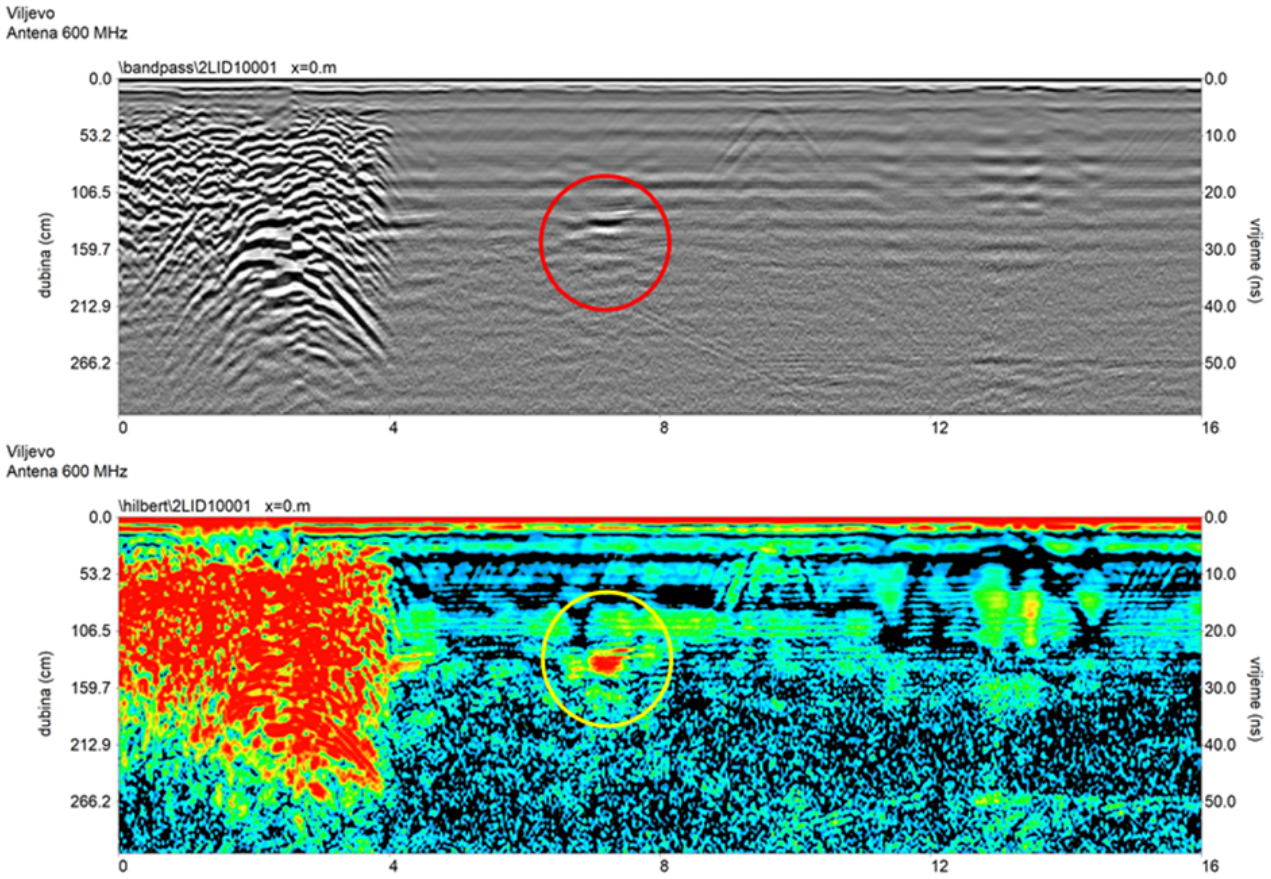

Figure 10. Anomaly at scan line No. 2 after Time-to-Depth conversion, bandpass filtering (**above**) and Hilbert transformation (**below**)—600 MHz antenna.

Also, interesting results were obtained while scanning the structural integrity of the walls. For this survey the high-frequency 2 GHz antenna was used. It was discovered that the walls have parts made of different material than the rest of the church (Figures 11 and 12), which may indicate that the material of an older church was used or that there were openings in the wall at some time in history.

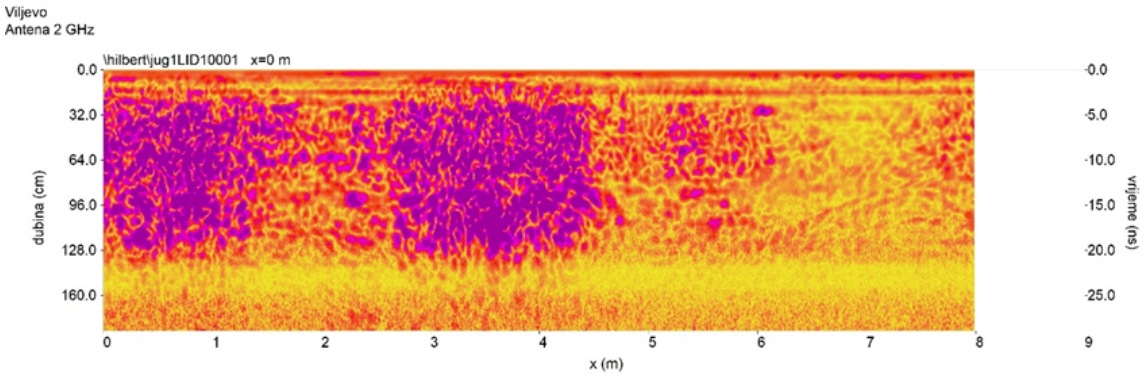

Figure 11. Radargram of the southern wall after Time-to-Depth conversion, bandpass filtering (**above**) and Hilbert transformation (**below**)—2 GHz antenna.

Figure 12. Southern wall with marked area made of different material.

4.3. Wastewater Treatment Facilities

The following example shows the determination of the existing reinforcement position and its protective layer in one of the facilities' reinforced concrete walls in Osijek, Croatia.

The survey of the span in the horizontal direction was carried out in five sections, and in the vertical direction it was carried out in two sections (Figure 13). The main vertical reinforcement in the upper zone is in some parts unevenly distributed (Figure 14). It is located at a depth of 21 to 76 mm and at average intervals of 10 cm (Figures 15 and 16).

Figure 13. The layout of the tested reinforced concrete wall with scan paths.

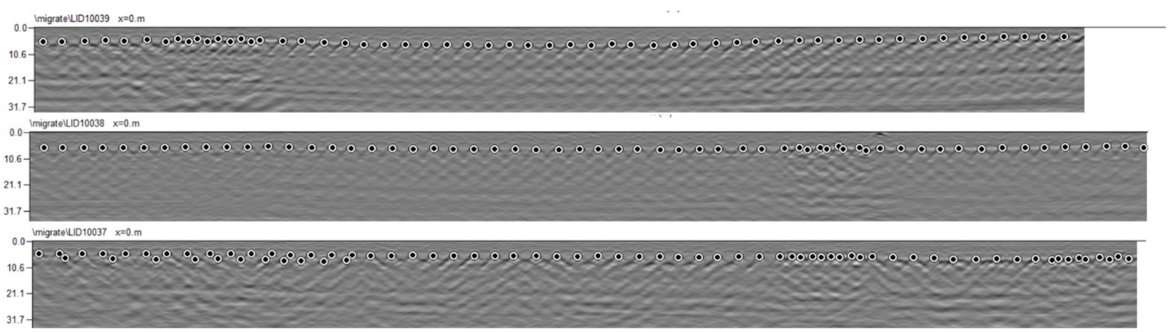

Figure 14. Radargrams of the wall, horizontal direction (Lines 1, 2, 3), 3.0 GHz antenna.

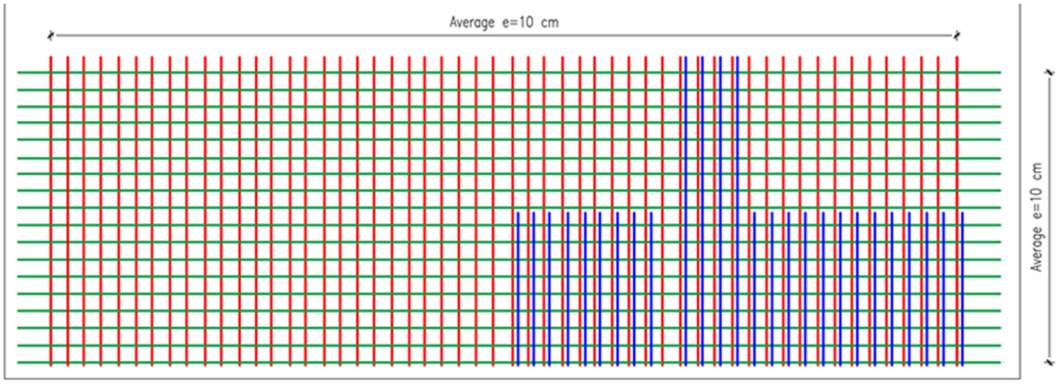

Figure 15. Plan view of test results: position of the horizontal and vertical reinforcement.

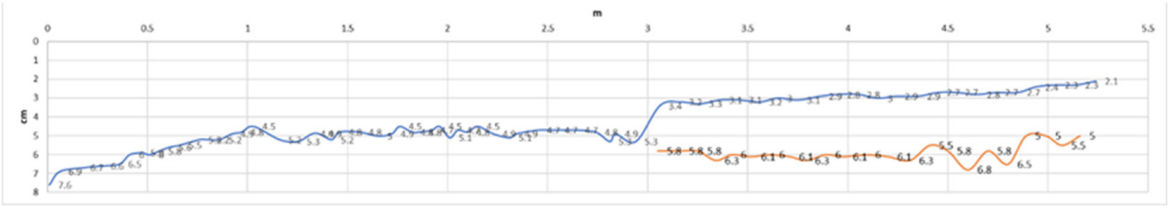

Figure 16. Protective layer of vertical rebars distribution, Line 1.

4.4. Reinforced Concrete Public Building in Subotica, Republic of Serbia

The following example shows the assessment of the corroded reinforcement in one of the building's reinforced concrete walls (Figures 17–19).

Figure 17. The layout of the tested reinforced concrete wall.

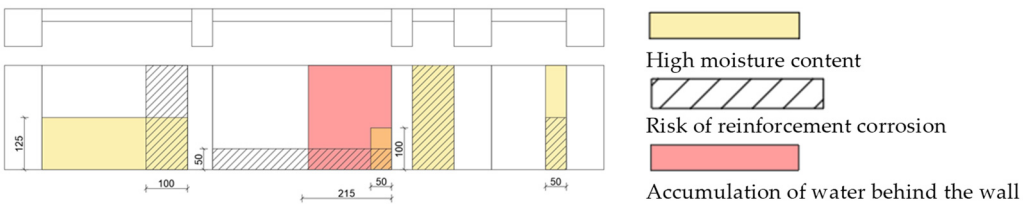

Figure 18. Various wet areas of the tested reinforced concrete wall.

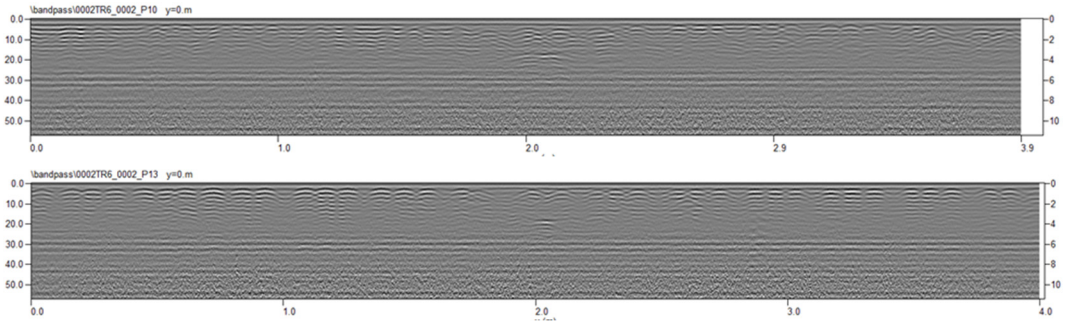

Figure 19. Characteristic radiograms of the tested rc wall, 3.0 GHz antenna.

5. Determination of the Dielectric Constant of Glued Laminated Timber Using Georadar

Georadar can be widely used in structural engineering to detect hidden defects within structural elements. It is used to find reinforcement bars and their position, cavities and cracks in concrete elements, as well as to detect the corrosion of bars. However, its application has been poorly investigated for glulam (Glue Laminated Timber—GLT) load-bearing elements. Glulam is a natural structural material made from laminates of timber glued together under heat and pressure. Such load-bearing elements have a high load capacity, do not have a problem with corrosion and have a high resistance to fire. The disadvantage of this material lies in its natural origin. In addition to being anisotropic, i.e., having different mechanical properties in different directions, it is subject to defects that can have a major impact on the load-bearing capacity. These defects can be cracks, knots, shakes or tunnel-like holes from insects. The detection of these irregularities within the structural element is of great importance, so georadar is an excellent solution. However, due to the size of these irregularities, which ranges from approximately 0.5 cm to 5.0 cm, the selection of the antenna, i.e., its central frequency, is particularly important. High frequency antennas (1 GHz and higher) must be used to detect such small targets.

The depth calibration is essential before data collection for an accurate investigation of any subsurface features. Thus, the effective dielectric property of any heterogeneous materials needs to be computed (calculated, simulated or measured), as the different proportions of varying material characteristics influence the geometric features of any considered material. The presence of air and water significantly affects the overall dielectric constant, as the presence of air reduces whereas that of water increases it. Therefore, velocity calibration becomes the primary source of errors if not performed appropriately and leads to unrealistic results that can have severe consequences. Once the dielectric constant of material is computed, the propagation velocity of the radar wave through that material can be determined according to Equation (2). As for the procedure, in our case, we used a practical approach. We did not analyze the antennas with the provided corresponding software for the results' analysis and interpretation. It was an iterative method where for an already known (measured) thickness of the specimen, a corresponding velocity and indirectly dielectric constant were measured and the new distance was calculated. This procedure was repeated until an acceptable error was achieved.

With that in mind, the main aim of this paper was to contribute or even improve the application of GPR in the testing of wooden structures, especially glue-laminated timber structures. The challenge here was an obvious high level of anisotropy of the material. Once determined, the dielectric constant values might now be used in a practical on-field test. However, what we also tried to investigate was the question of whether the frequency of the applied antenna might influence the results [21–23]. We found that it might, in our case especially with measurements tangential and perpendicular to the direction of the fibers.

5.1. About the Material

Glue-laminated timber (GLT or Glulam) is a structural engineering material used for load-bearing structural elements (Figure 20). It is produced from individual wood laminates, which are bonded together in one solid element. It is typically produced from spruce of fir wood, but other species may be used, such as pine, larch or poplar.

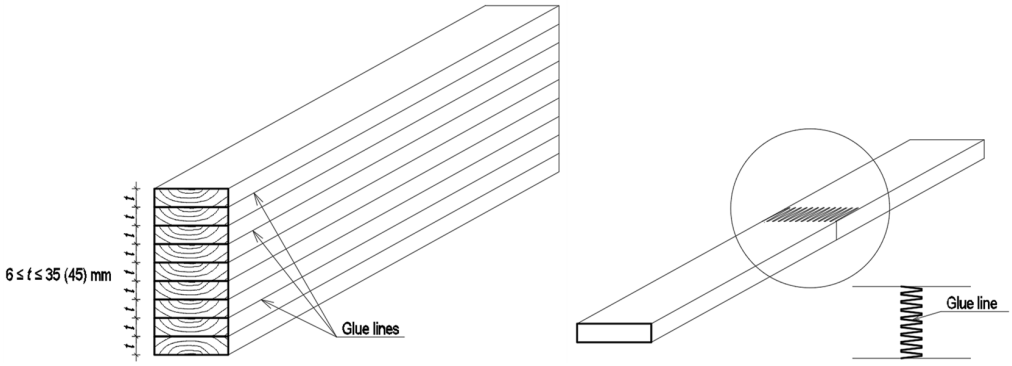

Figure 20. Glue-laminated beam and finger joint.

GLT structural members have many advantages: their small weight (around 400 kg/m^3) and finger joint technique allow spans of even up to 60 m, computerized production quality control ensures uniform characteristic mechanical properties and high strengths (up to 35 N/mm^2 for bending), and, contrary to common thinking, they have very good properties in fire conditions. Despite all these advantages, one should be aware that GLT is still a natural material and that it is susceptible to biological attack and damages caused by insects, fungi and bacteria. In addition, there is always the possibility of undetected inherited natural wood defects, such as knots, cracks and resin pockets. Therefore, it is very important to establish a reliable method of non-destructive testing of GLT elements in order to identify possible hazards to the structure over time.

5.2. Anisotropy of Wood

Glue-laminated timber (GLT or Glulam) is a structural engineering material used for load-bearing structural elements. It is produced from individual wood laminates, which are bonded together in one solid element. It is typically produced from spruce of fir wood, but other species may be used according to EN 14080 and EN 408, such as pine, larch or poplar.

As a natural building material, wood is far from being isotropic regarding its physical and mechanical properties. Three distinct anatomic axes of the wood may be observed in relation to these properties (Figure 21, left): longitudinal (L), transversal (T) and radial (R). Analogously, the mechanical properties of the wood, i.e., compression and tension strengths, differ in its perpendicular axes, depending on whether the stress is directed longitudinally or perpendicularly to the direction of the grains (Figure 21, right).

The figure on the right shows the change in wood strength depending on the direction of the fibers and the type of stress (pressure-tension). These strengths are directly related to the density of the wood. In the direction of the fibers, where the wood is densest, it can be seen that its strength, both in tension and pressure, is the highest, while it is lower perpendicular to the fibers. Such Mohr curves can be created for all anisotropic materials (such as concrete, for instance).

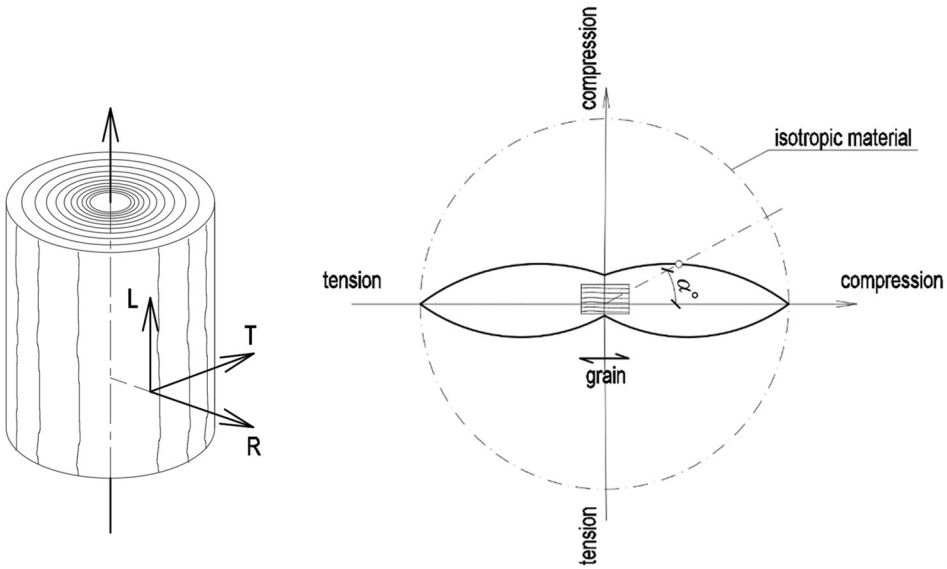

Figure 21. Anatomical axes of wood (**left**) and strength curve depending on the direction of the grains (**right**).

5.3. Test Setup

The tested GLT beam (Figure 22) was made of Central European fir wood (Abies alba) with dimensions of 17.9 × 47.2 × 180 cm. It consists of 12 lamellae 3.9 cm thick, bonded with melamine urea adhesive and hardener composed of formic acid and methanol. The adhesive and hardener are mixed with a ratio of 100:20 parts by weight. The thickness of the glue between lamellae is on average 0.3 mm (Figure 23). The electrical conductance of the adhesive is 280 µS, and that of the hardener is 14 µS. The moisture content in the GLT beam was measured at 20 locations along the specimen. The minimum moisture content was 7.1%, the maximum one was 7.9%, with an average of 7.46% with the most frequent value being 7.2%. The temperature of the room was 22°, and the humidity was 42%.

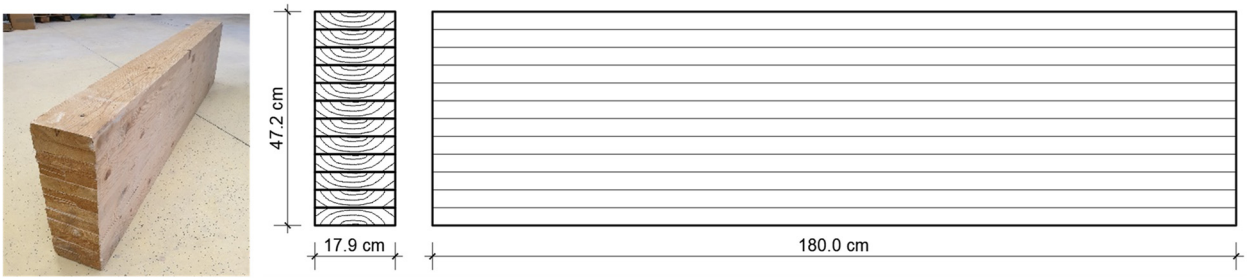

Figure 22. The tested GLT beam made of Central European fir wood.

Our main interest in this research was to observe how and to what extent the electromagnetic constant (that is, the electromagnetic wave speed) depends on the orientation of the wood fibers of the GLT beam and the main frequency of the particular antenna. Three antennas (Figure 24) were used, namely: 900 MHz, 2.0 GHz and 3.0 GHz. However, it is very important to mention that this dielectric constant largely depends on the type of wood and its humidity, but also on the wood origin (location).

The beam was placed on two powerful reflectors (steel plates), and the measurement was made in three mutually perpendicular directions (Figure 25). The main purpose of these steel plates at a known distance from the measuring surface (the height of the specimens, actually) was during the calibration of the measurement process. Thus, basically, instead of measuring the distances and layers with assumed dielectric constants or the propagation velocity of radar signals, velocities/dielectric constants were checked against a given/known distance (Figures 26 and 27).

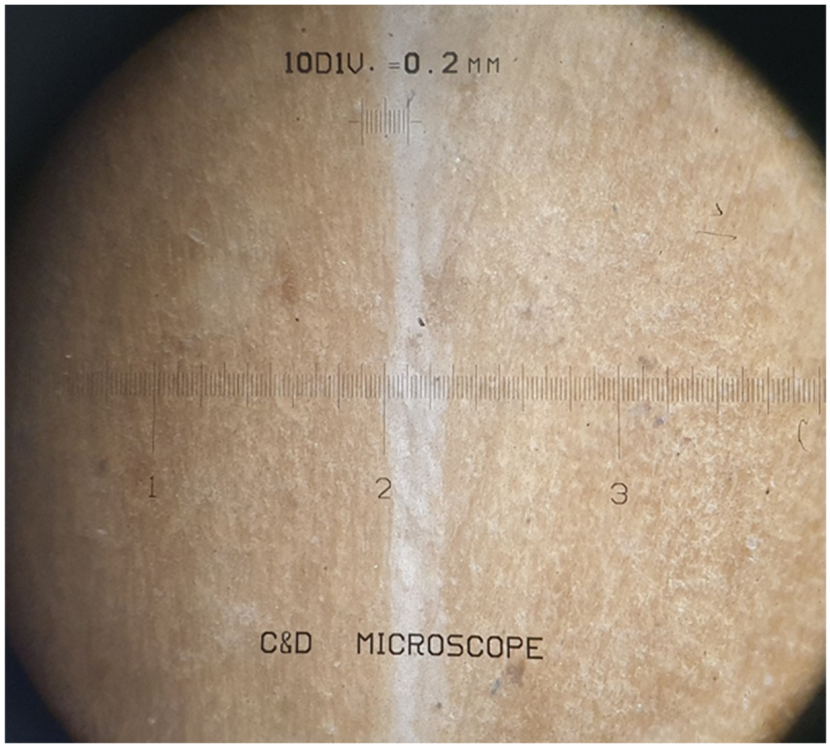

Figure 23. Thickness of the glue.

Figure 24. The test antennas: 900 MHz (**left**), 2.0 GHz (**center**), and 3.0 GHz (**right**).

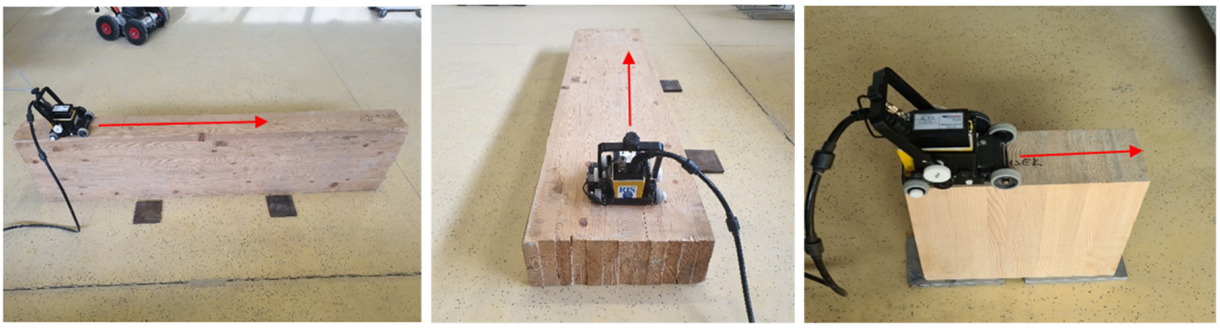

Figure 25. Measurements in the direction of the fibers (**left**), tangential to the direction of the fibers (**center**) and perpendicular to the direction of the fibers (**right**).

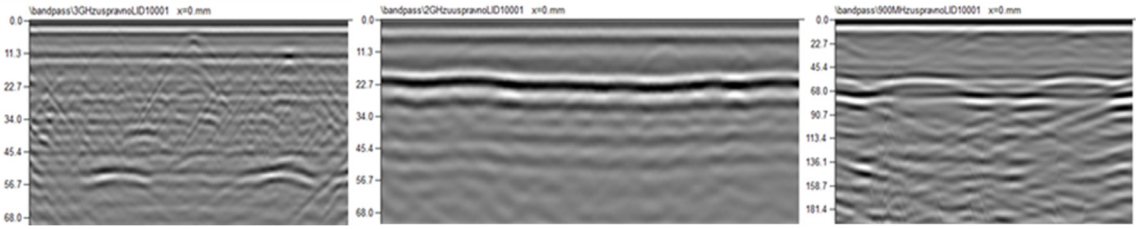

Figure 26. Radargrams obtained with 3.0 GHz, 2.0 GHz and 900 MHz test antennas (measurements in the direction of the fibers).

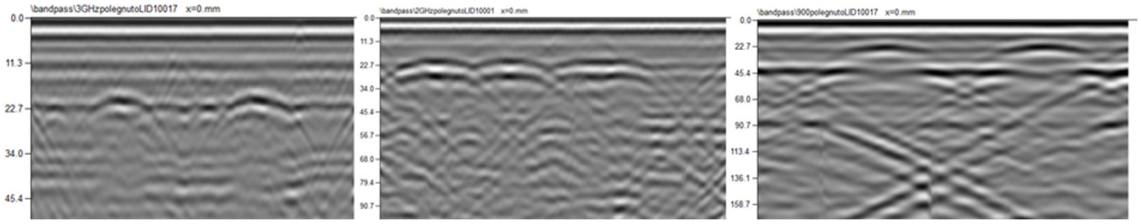

Figure 27. Radargrams obtained with 3.0 GHz, 2.0 GHz and 900 MHz test antennas (measurements tangential to the direction of the fibers).

5.4. Steps for Processing the Real Measured GPR Data

Raw data collected by field survey are saved as a series of individual radar traces (A-scan or time-amplitude scan) (Figure 28a) and are not suitable for interpretation. By processing successive radar traces from A-scan (Figure 28b), a more appropriate image (B-scan) (Figure 28c) is obtained, which can be visually interpreted. Basically, the amplitudes, positive and negative, are read from the radar traces and assigned a certain shade of color.

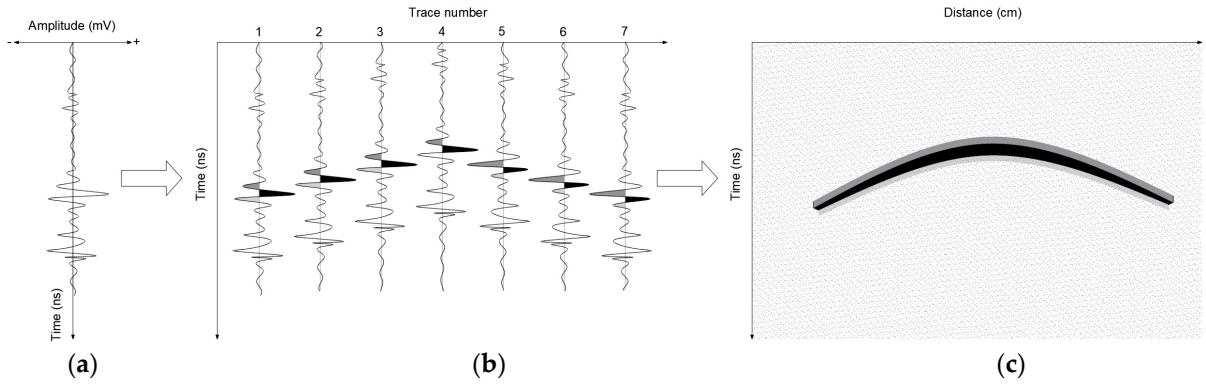

Figure 28. (**a**) A-scan; (**b**) assembling of consecutive A-scans; (**c**) B-scan.

Still, the B-scans generated in this way, apart from the data of interest, contain noise which comes from oscillating components that have a regular frequency. The bandpass filter removes redundant frequencies in the radar pulse that create noise and hide the target (Figure 29). Basically, this filter rejects frequencies outside a defined range. This range is user-defined and depends on the central frequency of the antenna, the characteristics of the medium and the target itself. There is no universal rule for determining the frequency range, but for each case, several variants should be tried until the most visible target is obtained.

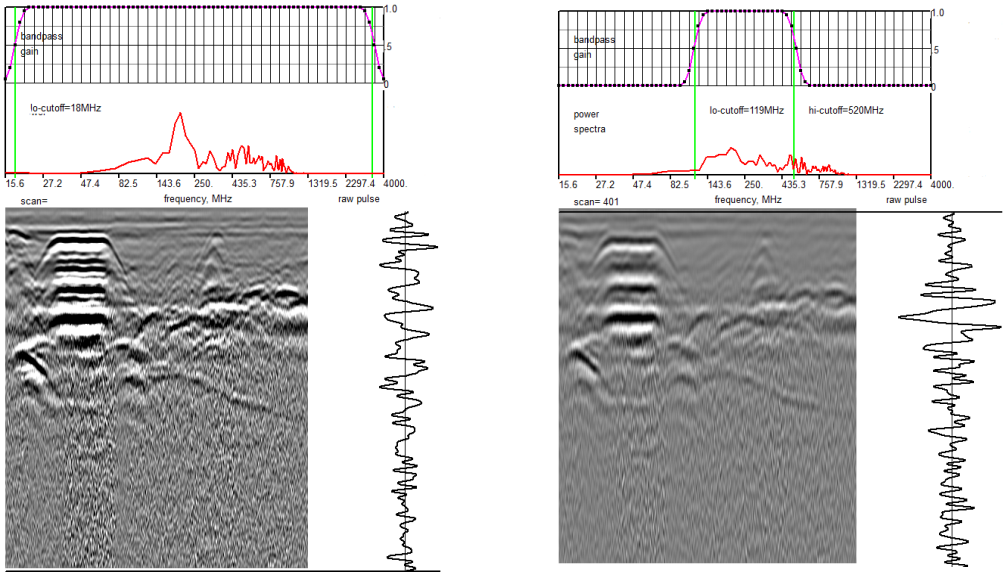

(**a**) (**b**)

Figure 29. From the row to the filtered images (schematic procedure). (**a**) Without bandpass filter. (**b**) With bandpass filter.

5.5. Test Results

The tested GLT beam (Figure 22) was made of Central European fir wood (*Abies alba*) with dimensions of 17.9 × 47.2 × 180 cm. It consists of 12 lamellae 3.9 cm thick, bonded with melamine urea adhesive and hardener composed of formic acid and methanol. The adhesive and hardener are mixed with a ratio of 100:20 parts by weight.

In this paper, we presented a case study using a methodological and data-processing approach for the assessment of structures using a high-frequency, and in the case of 2.0 GHz even dual-polarised, antenna system. The results have proven the advantages of using the proposed methodology and GPR system in order to improve the detectability of relatively small targets (Tables 4–6). However, since georadar measurements are carried out in situ, not in laboratory conditions and with specialized equipment, it is possible that certain deviations may appear due to signal dispersion and noise in the reflected wave. Moreover, the horizontal polarization was proven to be more stable compared to the vertical one, which is quite logical since the horizontal distance measurements are carried out by integrated electronic wheels. As for the eventual impact of a certain percentage of variation in the dielectric constant (3% in our case), one must keep in mind that here we are dealing with relatively very small targets. Thus, for instance, if we consider a 150 cm high structural member produced with glued laminated timber, 3% in vertical resolution produces limits of approximately 4.5 cm, which can exceed the size of the target.

Table 4. Results of measurements in the direction of the fibers.

Antenna	3 GHz	2 GHz	900 MHz
Dielectric constant, ε'	1.93	1.92	1.90
Bandpass filter	1400–4000 MHz	1000–3000 MHz	450–1500 MHz
Range	16 ns	32 ns	64 ns
Samples	512	512	512

Table 5. Results of measurements tangential to the direction of the fibers.

Antenna	3 GHz	2 GHz	900 MHz
Dielectric constant, ε'	1.95	1.59	1.75
Bandpass filter	1400–4000 MHz	1000–3000 MHz	450–1500 MHz
Range	16 ns	32 ns	64 ns
Samples	512	512	512

Table 6. Results of measurements perpendicular to the direction of the fibers.

Antenna	3 GHz	2 GHz	900 MHz
Dielectric constant, ε'	2.45	2.73	2.65
Bandpass filter	1400–4000 MHz	1000–3000 MHz	450–1500 MHz
Range	16 ns	32 ns	64 ns
Samples	512	512	512

The results of tests in the direction of the fibers showed the most consistency in measured values with negligible variations (1.90–1.93) with regards to the testing antenna used. As for the other two types of tests (measurements tangential and perpendicular to the direction of the fibers), the variations of the measured results with regards to the testing antenna used were more pronounced (up to 3%), indicating the necessity of considering not only the material's overall dielectric constant values but also the type (frequency) of antenna used. The results obtained were in accordance with those obtained in similar tests on timber structures [24,25].

The following figures show a comparison of the GPR raw data images and the processed B-scans (after the bandpass filter) for all three antennas, 900 MHz, 2.0 GHz and 3.0 GHz, with measurements in the direction tangential to the direction of fibers (Figures 30–32).

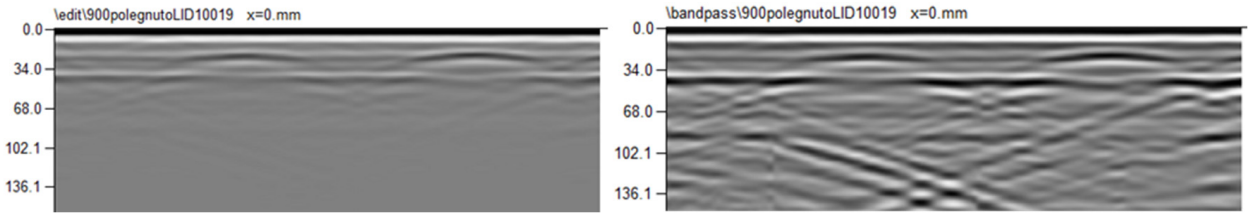

Figure 30. Raw-to-processed image with 900 MHz antenna.

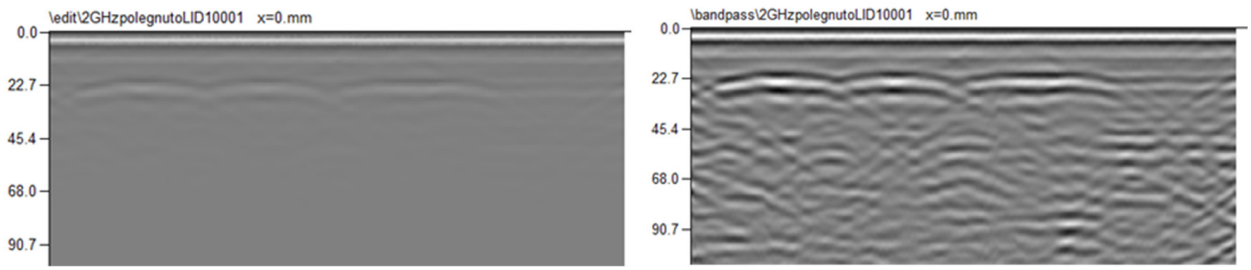

Figure 31. Raw-to-processed image with 2.0 GHz antenna.

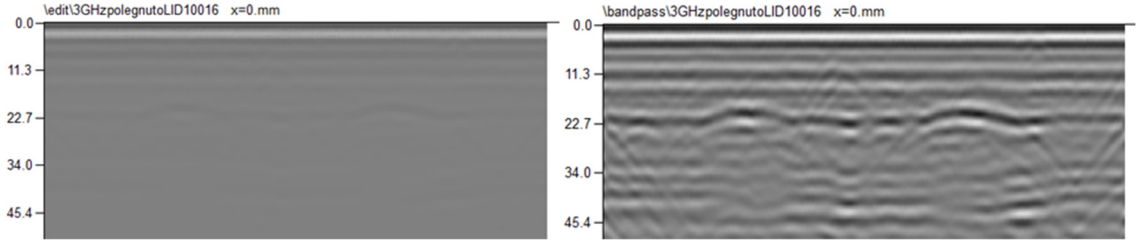

Figure 32. Raw-to-processed image with 3.0 GHz antenna.

6. Conclusions

Ground Penetrating Radar is powerful tool for many different applications. As a non-destructive technique, it has major advantages over other methods because it is fast and its results may be interpreted on site. The high-frequency antennas (1 GHz and above) can be very successfully used in structural engineering for detecting the reinforcement within the concrete body, cavities and layers of material. Moreover, as shown in this case study, through a carefully determined dielectric constant, it might serve in early defects detection inside bearing structures made of glued laminated timber, such as cracks, knots, shakes or tunnel-like holes from insects. Very often, as shown in the previous case studies, GPR provided critical data without which structural verification would not be possible. Despite all the advantages of the GPR, a potential user must be aware that this technique is not a "miracle tool" but that it also has serious disadvantages. The quality of data strongly depends on the type of the media and its assumed properties.

The presented case study used a methodological and data-processing approach for the assessment of structures using a high-frequency antenna system. The results have proven the advantages of using the proposed methodology and GPR system in order to improve the detectability of relatively small targets. However, since georadar measurements are carried out in-situ, not in laboratory conditions and with specialized equipment, it is possible that certain deviations may appear due to signal dispersion and noise in the reflected wave. Moreover, the horizontal polarization was proven to be more stable compared to the vertical one, which is quite logical since the horizontal distance measurements are carried out by integrated electronic wheels.

Considering all that, the main intention of this paper was to examine how and to what extent the electromagnetic constant (that is, the electromagnetic wave speed) depends on the orientation of the wood fibers of the GLT beam and the main frequency of the particular antenna. Our findings pointed out that except in the case of measurements in the direction of the fibers, the measurements tangential and perpendicular to the direction of the fibers might show slightly different results if an average dielectric constant is used, regardless of the measurement direction. Moreover, the same applies for the influence of the test antenna's frequency. Although these differences do not appear to be that significant, in cases of tests with high precision and better resolution demands, they might influence the actual results. The results (dielectric constants) obtained by tests in this case study are in conformity with similar tests made on timber materials and are in the range of 1.50 to 2.75, depending on the direction of the fibers.

Author Contributions: Conceptualization, D.V. and I.I.O.; methodology, I.G.; software, D.V.; formal analysis, I.G. and D.V.; testing, D.V., I.G., I.I.O. and D.R.; data curation, D.R.; writing—original draft preparation, D.V. and I.G.; writing—review and editing, I.I.O. and D.R.; visualization, D.V. and I.G. All authors have read and agreed to the published version of the manuscript.

Funding: This research received no external funding.

Data Availability Statement: Data are contained within the article.

Conflicts of Interest: The authors declare no conflicts of interest.

Nomenclature

Abbreviations	
GPR	Ground Penetrating Radar
EM	Electromagnetic
RC	Reinforced concrete
Symbols	
v	propagation velocity of EM wave in the media
c_0	EM wave velocity in vacuum ($3{\cdot}10^8$ m/s)
ε_r	relative permittivity
μ_r	relative magnetic permeability
σ	electrical conductivity
ω	angular frequency
ε	dielectric permittivity
P_{min}	minimum detectable power of the receiver
P_t	transmitter output power
E_t and E_r	antenna efficiency (transmitter and receiver, respectively)
G_t and G_r	antenna gain (transmitter and receiver, respectively)
f	central frequency of antenna
v_m	propagation velocity
α	attenuation coefficient of medium
g	scatter gain of target
σ	target scattering cross-section area
R	distance to the target
λ	wavelength
v	propagation velocity of EM wave in the media
f	central frequency of antenna

References

1. Benedetto, A.; Pajewski, L. *Civil Engineering Applications of Ground Penetrating Radar*; Springer Transactions in Civil and Environmental Engineering; Springer: Berlin/Heidelberg, Germany, 2015. [CrossRef]
2. Morey, R.M. *Ground Penetrating Radar for Evaluating Subsurface Conditions for Transportation Facilities*; Transportation Research Board, National Academy Press: Washington, DC, USA, 1998.
3. Walia, A.; Rastogi, R.; Kumar, P.; Jain, S.S. Reviewing methods for determination of Dielectric Constant required to Calibrate GPR Study for Asphalt Layers. *IOP Conf. Ser. Mater. Sci. Eng.* **2021**, *1075*, 012026. [CrossRef]
4. Mendoza, R.; Araque-Perez, C.; Marinho, B.; Rey, J.; Hidalgo, M.C. Processing GPR Surveys in Civil Engineering to Locate Buried Structures in Highly Conductive Subsoils. *Remote Sens.* **2023**, *15*, 4019. [CrossRef]
5. Prego, F.J.; Solla, M.; Puente, I.; Arias, P. Efficient GPR data acquisition to detect underground pipes. *NDTE Int.* **2017**, *91*, 22–31. [CrossRef]
6. Wai-Lok Lai, W.; Dérobert, X.; Annan, P.A. Review of Ground Penetrating Radar application in civil engineering: A 30-year journey from Locating and Testing to Imaging and Diagnosis. *NDTE Int.* **2018**, *96*, 58–78. [CrossRef]
7. Pajewski, L.; Fontul, S.; Solla, M. Ground-penetrating radar for the evaluation and monitoring of transport infrastructures. In *Innovation in Near-Surface Geophysics. Instrumentation, Application, and Data Processing Methods*; Elsevier: Amsterdam, The Netherlands, 2019; pp. 341–398.
8. Rathod, H.; Debeck, S.; Gupta, R.; Chow, B. Applicability of GPR and a rebar detector to obtain rebar information of existing concrete structures. *Case Stud. Constr. Mater.* **2019**, *11*, e00240. [CrossRef]
9. Solla, M.; Pérez-Gracia, V.; Fontul, S.A. Review of GPR Application on Transport Infrastructures: Troubleshooting and Best Practices. *Remote Sens.* **2021**, *13*, 672. [CrossRef]
10. Neto, P.X.; Medeiros, W.E. A practical approach to correct attenuation effects in GPR data. *J. Appl. Geophys.* **2006**, *59*, 140–151. [CrossRef]
11. Peng, Z.; Jing, G.; Wang, S.; Li, Y.; Guo, Y. Railway ballast layer inspection with different GPR antenas and frequencies. *Transp. Geotech.* **2022**, *36*, 100823.
12. Reppert, P.M.; Morgan, F.D.; Toksöz, M.N. Dielectric constant determination using ground-penetrating radar reflection coefficients. *J. Appl. Geophys.* **2000**, *43*, 189–197. [CrossRef]
13. de Aguiar, G.Z.; Lins, L.; de Paulo, M.F.; Maciel, S.T.R.; Rocha, A.A. Dielectric permittivity effects in the detection of tree roots using ground-penetrating radar. *J. Appl. Geophys.* **2021**, *193*, 104435. [CrossRef]
14. Ciampoli, L.B.; Tosti, F.; Economou, N.; Benedetto, F. Signal Processing of GPR Data for Road Surveys. *Geosciences* **2019**, *2*, 96. [CrossRef]

15. Forte, E.; Dossi, M.; Pipan, M.; Colucci, R. Velocity analysis from common offset GPR data inversion: Theory and application to synthetic and real data. *Geophys. J. Int.* **2014**, *197*, 1471–1483. [CrossRef]
16. Baker, G.S.; Jol, H.M. *Stratigraphic Analyses Using GPR*; Geological Society of America: Boulder, CO, USA, 2007.
17. Joshaghani, A.; Shokrabadi, M. Ground penetrating radar (GPR) applications in concrete pavements. *Int. J. Pavement Eng.* **2022**, *23*, 4504–4531. [CrossRef]
18. Chantasen, N.; Boonpoonga, A.; Athikulwongse, K.; Kaemarungsi, K.; Akkaraekthalin, P. Mapping the physical and dielectric properties of layered soil using short-time matrix pencil method-based ground-penetrating radar. *IEEE Access* **2020**, *8*, 105610–105621. [CrossRef]
19. Perez-Gracia, V.; Di Capua, D.; Gonzalez-Drigo, R.; Pujades, L.G. GPR resolution in NDT studies of structural elements: Experimental methodology and examples. In Proceedings of the NDTCE'09, Non-Destructive Testing in Civil Engineering, Nantes, France, 30 June–3 July 2009.
20. Carrick Utsi, E. *Ground Penetrating Radar: Theory and Practice*; Butterworth-Heinemann: Oxford, UK, 2017.
21. Revil, A. Effective conductivity and permittivity of unsaturated porous materials in the frequency range 1 MHz–1 GHz. *Water Resour. Res.* **2013**, *49*, 306–327. [CrossRef] [PubMed]
22. Antoine, R. Dielectric permittivity of concrete between 50 MHz and 1 GHz and GPR measurements for building materials evaluation. *J. Appl. Geophys.* **1998**, *40*, 89–94. [CrossRef]
23. Perez-Pena, M.; Roy, D.M.; Bhalla, A.S.; Cross, L.E. Dielectric properties of densified hardened cementitious materials. *Cem. Concr. Res.* **1986**, *16*, 951–965. [CrossRef]
24. Olmi, R.; Bini, M.; Ignesti, A.; Riminesi, C. Dielectric Properties of Wood from 2 to 3 GHz. *J. Microw. Power Electromagn. Energy* **2000**, *35*, 135–143. [CrossRef] [PubMed]
25. He, X.; Xie, J.; Xiong, X.; Li, Y.; Wei, Y.; Quan, P.; Mou, Q.; Li, X. Study on dielectric properties of poplar wood over an ultra-wide frequency range. *BioResources* **2017**, *12*, 5984–5995. [CrossRef]